Available online at www.sciencedirect.com
SCIENCE DIRECT®
Polymer 44 (2003) 4293–4300
polymer
www.elsevier.com/locate/polymer

Creep of PVDF monofilament sutures: service performance prediction from short-term tests

João F. Mano[a,b,*,1], João L. Lopes[c], Rui A. Silva[c], Witold Brostow[d,2]

[a]*Department of Polymer Engineering, University of Minho, Campus de Azurém, 4800-058 Guimarães, Portugal*
[b]*3B's Research Group—Biomaterials, Biodegradables and Biomimetics, University of Minho, Campus de Gualtar, 4710-057 Braga, Portugal*
[c]*ISEP—Instituto Superior de Engenharia do Porto, CIEA, R Dr António Bernardino de Almeida, 431 4200-072 Porto, Portugal*
[d]*Laboratory of Advanced Polymers and Optimized Materials (LAPOM), Department of Materials Science and Engineering, University of North Texas, Denton, TX 76203-5310, USA*

Received 23 April 2003; received in revised form 23 April 2003; accepted 30 April 2003

Abstract

Isothermal short-term creep of poly (vinylidene fluoride) (PVDF) monofilament sutures was determined at several temperatures between 10 and 90 °C under the stress of 10 MPa. Long term service performance was predicted for 10 decades of time. The compliance master curve as a function of time fits a hyperbolic sine equation. The temperature shift factor as a function of the temperature a_T (T) is accurately represented by a general equation based on free volume. A simple relationship between the two parameters of the equation is explored. The viscoelasticity of PVDF is also seen in dynamic mechanical analysis performed at the frequency of 1 Hz. The origin of the viscoelastic character well present in the deformability of the PVDF in service is due to the occurrence of the α_c relaxation that is active at ~50 °C (E'' peak at 1 Hz).

Keywords: Mechanical performance; relaxation behaviour; Biomedical applications

1. Introduction and scope

The interest in fluorinated polymers is closely connected to a number of their useful properties, including resistance to harsh environment, unique pyro- and piezo-electric characteristics [1–3] and also the capability to lower friction [4] and increase scratch resistance of thermosets [5]. Among fluoropolymers, polyvinylidene fluoride (PVDF), processable as a thermoplastic has a wide applications range from electronics to medicine—as a homopolymer, copolymer or blended with other polymers [3,6]. The versatility of PVDF in a wide range of applications has rendered this material certain popularity. When an alternative suture material turned out necessary, especially in vascular surgery, PVDF was presented to the medical device industry as a logical substitute for polyester [7] and polypropylene (PP)-both synthetic non-absorbable sutures.

The use and need for a suture should not be considered as a problem that needs solution, but rather as a solution that needs improvement. Dermatologic wounds can heal by themselves or—depending on the extension and depth—be closed by using a variety of methods. Notwithstanding the surgeon importance, the choice of the correct suture is fundamental for tissue healing and patient recovery. Usually, this choice takes into account the patient, the type of wound and tissue characteristics and also the anatomic region. The physical characteristics of a suture comprise the diameter, capillarity and hygroscopicity, tensile strength, knot strength, elasticity, plasticity, memory, and configuration. The configuration is based on the number of strands used to produce the suture, i.e. either single-stranded (monofilament) or multi-stranded (multifilament). For a long time, silk has been utilized as a non-absorbable suture (although it degrades within 24 months, when implanted), because of its softness and pliability. However, since it is a natural multi-filament, it can provide

* Corresponding author. Address: Department of Polymer Engineering, University of Minho, Campus de Azurém, 4800-058 Guimarães, Portugal. Fax: +351-253510339.
E-mail addresses: jmano@dep.uminho.pt (J.F. Mano), jll@isep.ipp.pt (J.L. Lopes), ras@isep.ipp.pt (R.A. Silva), brostow@unt.edu (W. Brostow).
[1] http://www.dep.uminho.pt/3bs.
[2] http://www.unt.edu/LAPOM/.

0032-3861/03/$ - see front matter © 2003 Elsevier Science Ltd. All rights reserved.
doi:10.1016/S0032-3861(03)00361-6

bacteria passage by capillarity, and hypersensitivity has been reported [8].

PVDF monofilament sutures exhibit a handful of characteristics that can make the difference: minimal tissue response and long-term stability in vivo, pliability and thus easy manipulation, and also the possibility of being sterilized by β or γ radiation instead of depending on ethylene oxide and chlorofluorocarbons [9]—thus more ecological.

PVDF sutures have also proven their good performance when compared to PP in tendon repair surgery. Even though the latter was considered as the material of choice for such medical procedure [10], PVDF monofilament sutures are becoming a growing alternative to the PP monofilament sutures [11].

Sutures are subjected to mechanical stresses when in use. Since we are dealing with viscoelastic materials, important information on their deformation is obtained by measuring *creep* under a constant stress [12]. Such results for sutures—and for that matter for any medical materials [13]—would allow to recognize fully the limits of service application of a given materials system and/or to develop improved materials for medicine. Note that in this case the more conventional quasi-static tensile tests, that provides typical stress/strain curves, gives dubious informations in the context of testing materials for long term load-bearing applications, as the experiments are performed too fast. At the same time, long-term performance of viscoelastic materials for medical uses needs to be connected to the microstructure (orientation, morphology, crystallinity), chemical structure (branching, cross-linking, molecular mass distribution) and also the total chemical composition including concentrations of additives when present.

In general, polymers are viscoelastic hence their properties change with time. For obvious reasons, laboratory tests are of short duration such as several hours while we need predictions of service performance and reliability for *years*. Fortunately, the so-called *correspondence principles* can be used for the purpose. The time–temperature correspondence (TTC) principle pioneered long ago by Ferry [14,15] tells us that short term isothermal tests at a number of temperatures can be used to predict long term behaviour at a chosen temperature. This is still often done using the so-called WLF equation of Ferry and co-workers proposed in 1955 [14]. As stated by Ferry [15], reliable values can then only be obtained between the glass transition temperature T_g and $T_g + 50$ K. Application of the WLF equation outside of that range leads to disastrous results [16]. However, using the chain relaxation capability (CRC) approach, a more general equation for such predictions has been developed by one of us [17–20]. It has provided good results in all cases it has been used [16–19,21–24]. The time–stress correspondence principle (TSC) first discovered experimentally in 1948 [25] can also be used for long term service performance prediction-particularly so since an equation based on it has been derived in 2000 [20] and used successfully [26,27]. The use of the CRC approach requires the knowledge of free volume v_f defined as

$$v_f = v - v^* \tag{1}$$

where v is the specific volume, in our case expressed in $cm^3\ g^{-1}$ and v^* is the characteristic (hard-core, incompressible) volume in the same units. In principle v^* is achieved at extremely high pressure and zero thermodynamic temperature conditions.

In the present work, we have performed creep experiments and used the CRC approach [17–19] including the TTC to predict long term behaviour of PVDF from short term tests. Apart from creep, an important technique for evaluation of viscoelasticity is the dynamic mechanical analysis (DMA) [28–30] where a sinusoidal load is imposed on the specimen and frequency as well as temperature are independent variables. DMA is already in use for medical materials [30] and we have also used it to advantage.

2. Experimental

2.1. Materials

PVDF 3-0 gauge blue tinted monofilament sutures developed by Laboratoire Pharmaceutique Péters (Bobigny, France) and commercially available under the tradename of Premio™ were investigated. The average diameters were determined by scanning electron microscopy (SEM) in 5 different locations for each sample and ranged from 240 to 269 μm. The average specific weight of the samples was $1.794 \pm 0{,}009\ g\ cm^{-3}$, determined by the Archimedes method using propanol at 20 °C.

2.2. Differential scanning calorimetry

DSC was performed with a Perkin–Elmer DSC7 apparatus. The temperature of the equipment was calibrated with indium and lead standards; the same indium sample was used for the heat flow calibration. The heating rate was $20\ K\ min^{-1}$.

2.3. Creep

The creep experiments were carried out in a Perkin–Elmer DMA7e apparatus using the tensile mode. This instrument controls the load applied to the top clamp and measures accurately (with the precision of ±50 nm) the distance between the clamps. Thus, DMA-7e is well suited for creep experiments. Continuous flux of high purity helium (flow rate of $\sim 28\ cm^3\ min^{-1}$) was used to improve heat transfer throughout the sample surroundings during the experiments. The sample length between the clamps was approximately 15 mm. A small load prior to the experiments was applied to the samples to provide a taut extension. The

creep stress level was $\sigma = 10$ MPa applied for 120 min at the following temperatures: 10, 30, 45, 55, 60, 70 and 90 °C.

2.4. Dynamic mechanical analysis

DMA was performed on our sutures in the temperature range from −55 to 140 °C at the frequency of 1 Hz, using also the Perkin-Elmer DMA7 apparatus. The stresses applied were small enough to assure that the mechanical response is within the linear viscoelastic regime [12,31]. Typical DMA results include the complex modulus

$$E^* = E' + iE'' \quad (2)$$

and the loss factor

$$\tan\delta = E''/E' \quad (3)$$

where E' is the storage (elastic, solid-like) modulus and E'' the loss (viscous flow, liquid-like) modulus.

2.5. Equation of state determination

Free volume as defined by Eq. (1) can be obtained from a set of $v = v(T, P)$ results using an equation of state where P is the applied pressure. An apparatus for that purpose called Gnomix has been developed already decades ago by Zoller and co-workers [32] and recently used with good results [33,34].

The sample with the weight between 0.5 and 2.5 g of *any* shape is first dried under vacuum for several hours and then placed in a rigid cell with flexible bellows at the bottom and degassed again. The volume that is not taken by the sample is filled by mercury under vacuum. The cell is installed inside a pressure vessel in which pressures up to 240 MPa and temperatures up to 400 °C can be controlled. The deflexion of the bellows resulting from changes in temperature or pressure is measured with a linear variable differential transducer. These deflections are converted into volume changes of the sample proper on the basis of well-established P–V–T properties of mercury.

3. Differential scanning calorimetry results

Both first and second consecutive DSC scans for a PVDF sample are shown in Fig. 1. Melting of the crystalline fraction only is observed in the temperature region studied. From polarised light microscopy no spherulitic morphology was detected; instead an oriented semi-crystalline structure induced during fibre processing is visible.

The melting enthalpies for the first and second scans are $\Delta H_m = 56.0$ and 49.4 J g^{-1}, respectively. If we take the value for fully crystalline PVDF as $\Delta H_{m,100\%} = 104.7$ J g^{-1} [35], the percentage degree of crystallinity of a semi-crystalline sample calculated as $100\Delta H_m/\Delta H_{m,100\%}$ gives for the two runs, respectively, 53.5 and 47.2 %. The lower value in the second scans indicates that the stretching during processing of PVDF monofilaments enhances the crystallinity. Increasing the temperature during the scan resulted in a partial return to the unstretched amorphous state. The quiescent crystallisation which takes place between the first and the second heating runs-resulting mostly in formation of isotropic spherulitic structures-does not restore the initial crystallinity degree.

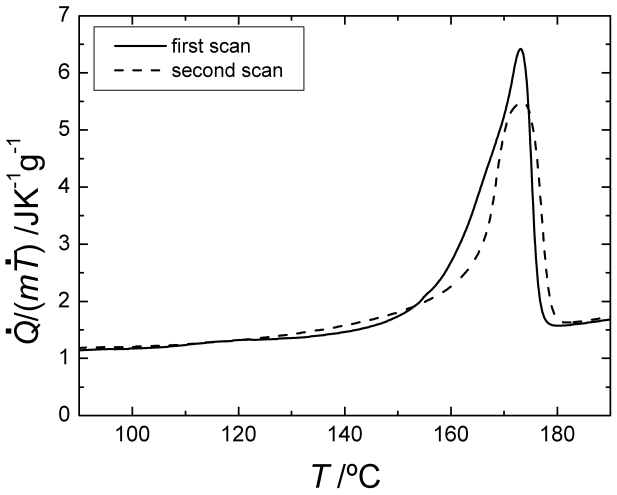

Fig. 1. DSC scans on 13.817 mg of the PVDF fibres obtained at 20 °C min^{-1}. The heat flux, $\dot{Q} = dQ/dt$, is normalised with the mass, m, and the heating rate, dT/dt. The first and the second scans on the same sample are shown (solid and dashed lines, respectively).

A shoulder in the low temperature side of the melting peak observed in the first scan seems to disappear during the second scan. This indicates the existence of thin lamellar structures that after melting are not re-created again during quiescent crystallisation. In fact, the second scan exhibits a narrower peak, mainly due to the disappearing of the low temperature shoulder. This is easily visualised in Fig. 1 and is also consistent with the increase of the onset temperature of the melting peak, from 163.0 to 164.4 °C between the first and the second DSC scans.

4. Equation of state results

P–V–T determinations with the Gnomix apparatus result typically in several hundreds of $v = v(T, P)$ values and need to be represented by an equation of state. Good results have been obtained repetitively [16,22–24,26,27,36] using the Hartmann equation of state [37,38]:

$$P_r v_r^5 = T_r^{3/2} - \ln v_r \quad (4)$$

where the reduced quantities are defined as

$$v_r = v/v^*, \qquad T_r = T/T^* \text{ and } P_r = P/P^* \quad (5)$$

v^* has already appeared in Eq. (1); T^* is proportional to the strength of intermolecular (in polymers intersegmental) interactions; P^* is a complicated function of the intersegmental or intermolecular potential $u(R)$ where R is the

distance and of the material structure represented by the binary radial distribution function $g(R)$ [39].

Thus, our 350 or so $v(T,P)$ datasets have been inserted into Eqs. (4) and (5) and solved for three unknowns, v^*, T^* and P^*. We have used a Levenberg–Marquart least square algorithm (JMP Version 4, Minneapolis, MN, USA) The results are: $v^* = 0.502\ \mathrm{cm^3\ g^{-1}}$; $T^* = 1624$ K; $P^* = 9.04$ GPa.

Our results can be compared with those for other semi-crystalline polymers. For instance, for PP [24] we have $v^* = 0.910$ $T^* = 876$ K; and $P^* = 3.90$ GPa. For polyethylene (PE) [22] we have $v^* = 0.930\ \mathrm{cm^3\ g^{-1}}$ and $T^* = 1221$ K. Thus, the incompressible volume v^* of the PVDF is significantly smaller than those of PE and PP. We infer that the relatively strong interactions between H and F atoms in PVDF result in a compact structure—leading to low v^* and high T^*. Our conclusion is confirmed by the fact that the density of PVDF is ≈1.80, of PE ≈0.93 and of PP ≈0.90 $\mathrm{cm^3 g^{-1}}$ [40].

5. Creep results

The creep results can be well represented by compliance D which is the measure of the ease with which the material deforms. Specifically

$$D(t) = \varepsilon(t)/\sigma_0 \tag{6}$$

where σ_0 is the constant static engineering stress applied to the specimen during creep and ε is the engineering strain (not to be confused with true strain) [41]. In the linear viscoelastic regime D is only a function of temperature and time. We have determined the time dependence of creep compliance D as a function of logarithmic time of the PVDF monofilaments at several temperatures. The results are shown in Fig. 2.

The curves displayed in Fig. 2 cover each two decades of time. The long term prediction we need is achieved by shifting all isothermal curves like those in Fig. 2 along the time axis until they form a single curve [15,19,20]. This approach is based on the TTC discussed in the Introduction and is also known as the method of reduced variables. For the compliance it implies that

$$D(t, T, \sigma_0) = D(t/a_T, T_{\mathrm{ref}}, \sigma_0) \tag{7}$$

where the reducing parameter a_T is called the temperature shift factor. T_{ref} is the temperature for which we are making the long term prediction (no shift) creating the so-called master curve.

The results of this operation are shown in Fig. 3; in our case $T_{\mathrm{ref}} = 30$ °C. We have thus obtained creep predictions for that temperature for nearly 10 decades of time. In literature, one talks sometimes about 'rheologically complex materials' to which TTC des not apply. However, as discussed in the Section 1, in a number of cases one applies the WLF equation outside of its validity range, obtains bad results as expected, and wrongly concludes that TTC does not apply. The conventional wisdom is that multi-phase materials are 'rheologically complex'. This is not true either; good results have been obtained on the basis of TTC and the CRC approach (see more below) for polymer liquid crystals which form four coexisting phases [16,23,24,26,27].

The master curve in Fig. 3 can be represented by an analytical equation. We have used [42]

$$\varepsilon(t) = \sinh\frac{\sigma_0}{\sigma_a} + \left(\frac{t}{t_0}\right)^n \sinh\frac{\sigma_0}{\sigma_b} \tag{8}$$

where σ_a, σ_b, n and t_0 are adjustable parameters. As argued by Turner [42], Eq. (8) combines the power law for the time dependence with the non-linearity with respect to the stress.

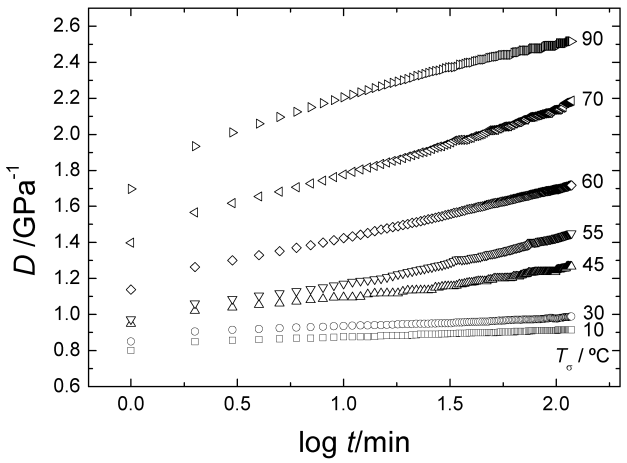

Fig. 2. Experimental creep compliance for the studied PVDF fibres as a function of log time at different creep temperatures, T_σ, between 10 and 90 °C (indicated in each results).

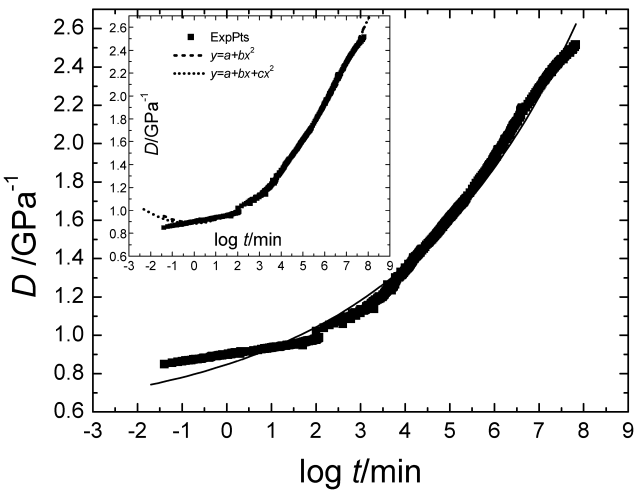

Fig. 3. The master curve of the studied PVDF fibres of creep compliance D for $T_{\mathrm{ref}} = 30$ °C, obtained from horizontal shiftings of the curves in Fig. 1. Points are experimental values and the solid curve is the non-linear fitting of the data with Eq. (8). The inset graphics shows the fitting of the same experimental points to the functions, $y = a + bx^2$ and $y = a + bx + cx^2$, where $y = D$ and $x = \log t$.

We have used again a Levenberg–Marquart least square algorithm but this time as implemented in Origin® 6.0 by Microcal Software, Northampton, USA. With a large number of experimental points, good convergence was achieved; the final values did not depend on the initial guesses, for the best case we have obtained the correlation coefficient $R^{2=}0.991$ ($\chi^2 = 2.5 \times 10^{-7}$). Since results for only one stress were used there is a dependence between the σ_b and t_0 parameters and only σ_a, and n can be directly obtained. The results are $t_0^{-n}\, sinh(10/\sigma_b) = 0.00311 \pm 0.0001$ (with σ_b in MPa and t_0 in minutes), $\sigma_a = 1860 \pm 35$ MPa and $n = 0.106 \pm 0.001$. Mechanical testing at several σ levels would be needed in order to obtain each of the four parameters independently of the other ones. The results obtained using Eq. (8) are shown as a thin curve in Fig. 3. There are reasonable results in the central part but clear deviations at the lower end—a surprising result for an equation with four parameters. The high value of the R^2 coefficient is clearly due to the large number of points in the central part.

We have also used simple polynomials, $y = a + bx^2$ and $y = a + bx + cx^2$ (with $y = D$ and $x = \log t$) previously used in the representation of creep data [24,27]. Last-square fits of the creep master curve with these two expressions are shown in the insert in Fig. 3. For long times region the agreement with experiment is quite good and similar results are obtained for the two equations. However, for short times physically unrealistic minima are seen in both curves. Thus, neither the polynomials nor Eq. (8) provide reliable results in the entire time scale range. Such models may still be useful to perform simple interpolations. We need, however, to consider now computation procedures which have a better physical basis.

For this purpose, we return now to the temperature shift factor a_T featured in Eq. (7)—clearly the key property that rescales the viscoelastic behaviour along the time axis for isothermal results other than those for the reference temperature T_{ref}. Experimental values of a_T ($T_{ref} = 30$ °C) are plotted as a function of temperature in Fig. 4 (squares).

We now need an analytical equation to represent $a_T(T)$. The WLF equation for a_T was mentioned, but we know it works only inside a specific narrow temperature interval. Arrhenius type equations with the so-called apparent activation energy E_a in the exponent are also in use. However, an analysis of creep and DMA data for high-density PE shows that E_a depends on the technique used to determine it—in spite of the same molecular mechanism manifesting itself in different experiments [36]. Moreover, it was pointed out [36] that E_a could strongly depend upon, for example, the degree of branching in PE-vitiating the physical basis of the Arrhenius model.

Molecular processes in polymeric materials, for instance those that involves conformational changes, require free volume defined by Eq. (1). Note that high values of v_f at elevated temperatures enable conformational processes to occur faster than at lower temperatures. Therefore, v_f is

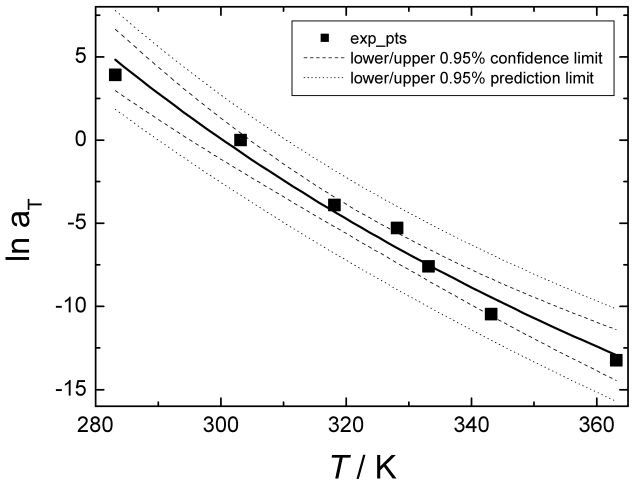

Fig. 4. The temperature shift factor for the studied PVDF fibres for $T_{ref} = 30$ °C (squares), obtained during the construction of the master curve in Fig. 2. The solid line is the non-linear fitting of the data with Eq. (7). The lower and upper confidence and prediction band curves are also shown in the graphics, both obtained for a confidence level of 95%.

intrinsically associated with the time–temperature correspondence principle. These facts lie at the foundation of the already mentioned CRC approach [17–20] which leads to the following equation for $a_T(T)$ [17,18]:

$$\ln a_T = A + B/(v_r - 1) \tag{9}$$

where A and B are constants characteristic for a given viscoelastic material; B is the Doolittle constant which originates from the seminal Doolittle equation relating viscosity to free volume [43]. While temperature T does not appear in Eq. (9) explicitly, it is represented by the reduced volume v_r that can be calculated from an equation of state. As already noted, we use the Hartmann Eq. (4) for the purpose. Eq. (9) is a special case of a more general equation for $a_{T,\sigma}$ [20] which relates shifting to both T and the stress level σ. In turn, by making a primitive (and unfounded) assumption, one obtains from Eq. (9) the old WLF equation as a special case.

Since our experiments were conducted at the atmospheric pressure ($P \approx 0.1$ MPa), the term containing P_r in Eq. (4) becomes negligible, and we obtain a simpler relationship:

$$v_r = \exp(T_r^{3/2}) \tag{10}$$

Substituting the last result into Eq. (9) we obtain

$$\ln a_T = A + \frac{B}{\exp[(T/T^*)^{3/2}] - 1} \tag{11}$$

The experimental data in Fig. 4 were represented by Eq. (11) using $T^* = 1624$ K (see above Section 4) and performing a non-linear regression. The resulting parameters are $A = -50.1 \pm 3$ and $B = 4.15 \pm 0.3$. The best fitted curve with $R^2 = 0.98$ ($\chi^2 = 0.82$), is shown in Fig. 4 as the solid line. Given the accuracy of the shifting

procedure, a satisfactory concordance between the experimental points and the calculated curve is achieved.

The parameter A can be related to microstructural characteristics of the system such as orientation [22]. The Doolittle parameter B is a true materials constant; the same value of B has been obtained for a polymer liquid crystal from temperature shift and stress shift experiments [26]. A review of previously reported A and B values, shows in certain cases an approximately relationship: $A = -10B$. This kind of compensation in kinetic-like models has been observed in other contexts, such has in the Arrhenius description of thermally stimulated processes, where a linear relationship is found between the pre-exponential and the activation energy [44]. A trial was performed assuming $A = -10B$ and fitting again the results with the Doolittle parameter only. However, attractive as this would be, the resulting curve presented large deviations from the experimental data.

Our results show once again the applicability of the CRC approach and of the equations based on it. This strengthens the applicability of the model to semi-crystalline polymers and provides some physical insights into interactions in the undeformed material and the deformation during creep.

With the information obtained, one can obtain the temperature dependence on the creep compliance at-for example-the physiological temperature of 37 °C. In this case, we find that $a_{37°C} = -2.46$, indicating that for 37 °C the curve in Fig. 3 should be displaced horizontally through the left-hand side by the amount of 2.46 along the log t axis.

6. Dynamic mechanical analysis

It is known that the energy furnished to a system, U_0 (impact or creep load, for example) may be either utilized in irreversible damage processes, such as bond breaking (with an energy U_b) or plastic deformation or dissipated in non-destructive and reversible processes [11]. Such dissipation in viscoelastic materials is largely related to relaxation processes and thus this term could be written as U_r. If U represents the part of input energy that did not go into either the two competitive processes, we may write [18]:

$$U = U_0 - U_b - U_r \tag{12}$$

The previous creep results suggest a clear viscoelastic character of the studied monofilaments when subjected to a static load, due to the observed time-dependent mechanical behaviour. Therefore, at the studied temperature region and at the time scale of the creep experiments, we may conclude that some relaxation mechanism is associated with the deformation process observed. It should be then important to clarify this mechanism at the molecular level, which will highly determine the mechanical performance of such material in service.

DMA is a suitable technique that allows for the viscoelastic characterisation of polymeric systems. In this work DMA experiments at constant frequency were performed while the temperature was scanned from −55 up to 140 °C. Fig. 5 shows the dependence of the storage modulus, E', the loss factor, tan δ, and the loss modulus, E'' (inset graphics), in this temperature region.

A maximum in tan δ is detected at $T \approx -40$ °C. This relaxation process, also detected by dielectric methods, has been labelled β or α_a. It has been assigned to the cooperative segmental motions within the main chains of the amorphous regions [45,46]. It should be noticed that at service temperature and for reasonable times, the molecular motions assigned to this process are completely relaxed. Therefore the segmental mobility of the amorphous phase does not contribute for the creep behaviour observed in the studied system. It will determine obviously the (instantaneous) elastic properties of the monofilament sutures, that are found to be much less stiffer at service conditions than, for example, at temperatures below −60 °C (see the strong decrease in E' in the low temperature region of Fig. 5).

At higher temperatures ($T > 0$ °C) a new relaxation emerges (Fig. 5). This process, labelled α or α_c, is associated with motions within the crystalline fraction, detected by DSC (Fig. 1) [45,46]. This higher $-T_g$ relaxation is also found in a variety of flexible semi-crystalline polymer, including PE, poly(methylene oxide), poly(ethylene oxide) and isotactic PP [47,48] and its origin should be similar to the one observed in PVDF. This relaxation is not clearly observed as a peak in the tan δ plot, although the damping capability of the system is significant (tan δ reaches values clearly above 0.1). This α_c-relaxation was also found, with similar features, in β-PVDF [49]; this material has a special crystalline arrangement that is responsible for its piezo- and piroelectric properties. It should be noticed that, despite no peak is found in tan δ, E'' presents a maximum at ~60 °C, compatible with the inflexion in the E' curve. The position in the temperature axis of the α_c-relaxation was found to be dependent on the crystalline morphology, namely the lamellae thickness [47].

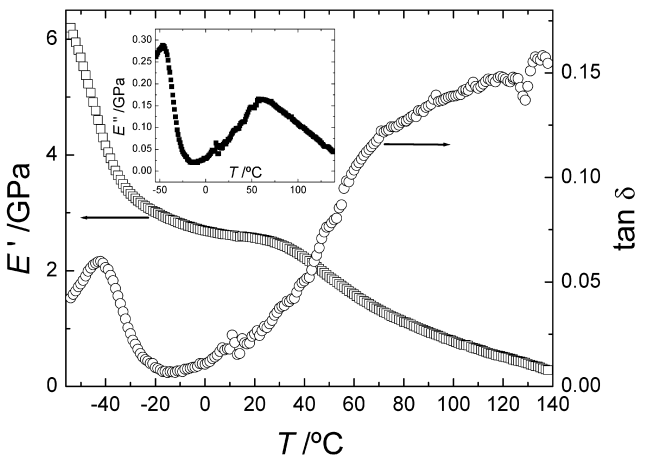

Fig. 5. DMA spectra at 1 Hz for the studied PVDF fibres (storage modulus, E', and loss factor, tan δ). The inset graphics shows the temperature dependence of the loss modulus, $E'' = E'$ tan δ.

As for PE, the α_c-relaxation process in PVDF should also involve 180° flip motions of the chain stems in the crystalline lamellae [47,48,50]. This screw motion process involves both a translation of one $-CH_2-$ unit and a rotation such that the portion of the chain in the crystallites is in its energetically most favourable position in the lattice before and after the jump rotational and translation mobility within the chains [51]. A significant cooperative character was found for PE, indicating that diffusion processes involving chains in the amorphous region should accompany the α_c-relaxation [52]; in fact, this processes emerges mechanically from an additional shear of the amorphous regions that needs to occur in order to provide the chain transport through the lamellae [47,48]. A similar degree of cooperativity was also found for the α_c-relaxation of PVDF [53], strengthening the attribution of the α_c-relaxation in PVDF and in PE to the same origin at the molecular level.

The α_c-relaxation influences the solid-state rheological features of PVDF above and near room temperature. In fact, if we consider the time scale of creep experiments, say from $\sim 10^1$ to 10^3 s then, for correct comparison, the corresponding dynamic experiments should be done at angular frequencies of 10^{-3} to 10^{-1} s^{-1}. Taking the frequency-temperature superposition principle, this would correspond to shift all the DMA data towards lower temperatures. Therefore, in the region of room temperature the material should exhibit considerable damping and dissipative capability, as the broad α_c-relaxation would be highly effective. These finding are then compatible with the previous creep results, that clearly shown a time-dependent deformation behaviour. At the molecular level, the changes in strain observed in the creep behaviour should have similar origin to the α_c-relaxation, i.e. they should assigned to screw-like motions in the crystalline phase accompanied with cooperative conformational changes within the amorphous phase. Similar relationships between creep and DMA experiments were discussed in the context of high-density PE [36]. In this case, it was found, for example, that the A and B parameters of Eq. (9) were similar using the temperature shift factors obtained from both mechanical methods. Also in this case the α_c-relaxation dominated the viscoelastic character of the material as probed by creep and DMA.

7. Concluding remarks

Creep experiments were found to be a suitable method to analyse the mechanical behaviour of PVDF monofilament sutures. Using the time–temperature superposition principle it was possible to predict the long-term deformation feature from short-term tests. A clear viscoelastic character of the sutures is seen. The kinetics of the molecular mobility was studied by adjusting the temperature shift factor with a model based on the free volume concept.

DMA tests allowed to detect in this materials two main relaxations: the β process, assigned to segmental mobility in the amorphous phase, and the α_c-relaxation, that is mainly a consequence of conformational motions within the crystalline fraction. The α_c-relaxation process will be the main source for energy dissipation that is input to the system during constant mechanical loading. In fact, at 1 Hz this process shows a maximum of E'' at ~60 °C, which would shift towards body temperature at time-scales of service conditions (hours to months).

The main findings of this paper and general methodologies employed are fairly general and may be applied in other PVDF suture formulations, and even in PP sutures; in fact, PP also exhibits similar relaxation features of PVDF (although shifted to higher temperatures), with the β and the α_c processes appearing at ~0 and ~100 °C, respectively [54].

Acknowledgements

We acknowledge the participation of Dr Gonzalo Martinez-Barrera and Miss Julie Plemons in the equation of state experiments. JFM acknowledges FCT for financial support.

References

[1] Cassidy PE, Aminobhavi TM, Farley JM. J Macromol Sci Rev C 1989;29:365.
[2] Laroche G, Marois Y, Schwarz E, Guidoin R, King MW, Pâris E, Douville Y. Artif Organs 1995;19:1190.
[3] Das-Gupta DK. Ferroelectrics 1981;33:75.
[4] Brostow W, Cassidy PE, Hagg HE, Jaklewicz M, Montemartini P. Polymer 2001;42:7971.
[5] Brostow W, Bujard B, Cassidy PE, Hagg HE, Montemartini PE. Mater Res Innovat 2002;6:7.
[6] Linares A, Acosta JL. Eur Polymer J 1997;33:467.
[7] Laroche G, Marois Y, Guidoin R, King MW, Martin L, How T, Douville Y. J Biomed Mater Res 1995;29:1525.
[8] Kurosaki S, Otsuka H, Kunitomo M, Koyama M, Pawankar R, Matumoto K. J Nippon Med Sch 1999;66:41.
[9] Urban E, King MW, Guidoin R, Laroche G, Marois Y, Martin L, Cardou A, Douville Y. ASAIO J 1994;40:145.
[10] Wada A, Kubota H, Hatanaka H, Miura H, Iwamoto Y. J Hand Surg 2001;26B:212.
[11] Laroche G, Lafrance CP, Prud'homme RE, Guidoin R. J Biomed Mater Res 1998;39:184.
[12] Goldman AY. In: Brostow W, editor. Performance of plastics. Munich: Hanser; 2000. Chapter 7.
[13] Shoichet MS, Hubbell JA. Polymers for tissue engineering. Utrecht: VSP; 1998.
[14] Williams ML, Landel RF, Ferry JD. J Am Chem Soc 1955;17:3701.
[15] Ferry JD, 3rd ed. Viscoelastic properties of polymers, New York: Wiley; 1980.
[16] Brostow W, D'Souza NA, Kubat R, Maksimov J. J Chem Phys 1999; 110:9706.
[17] Brostow W. Mater Chem Phys 1985;13:1741.
[18] Brostow W. In: Brostow W, Corneliussen RD, editors. Failure of plastics. Munich: Hanser; 1986. Chapter 10.

[19] Brostow W. In: Brostow W, editor. Performance of plastics. Munich: Hanser; 2000. Chapter 5.
[20] Brostow W. Mater Res Innovat 2000;3:347.
[21] Brostow W, Duffy JV, Lee GF, Madejczyk K. Macromolecules 1991; 24:479.
[22] Boiko YM, Brostow W, Goldman AY, Ramamurthy AC. Polymer 1995;36:1383.
[23] Brostow W, D'Souza NA, Kubat J, Maksimov R. Intranet J Polym Mater 1999;43:233.
[24] Akinay AE, Brostow W, Castaño VM, Maksimov R, Olszynski P. Polymer 2002;43:3593.
[25] O'Shaughnessy MT. Text Res J 1948;18:263.
[26] Akinay AE, Brostow W, Maksimov R. Polymer Eng Sci 2001;41:977.
[27] Akinay AE, Brostow W. Polymer 2001;42:4527.
[28] Menard KP. Dynamic mechanical analysis—a practical introduction. Boca Raton: CRC Press; 1999.
[29] Menard KP. In: Brostow W, editor. Performance of plastics. Munich: Hanser; 2000. Chapter 8.
[30] Mano JF, Reis RL, Cunha AM. Dynamic mechanical analysis in polymers for medical applications. In: Reis RL, Cohn D, editors. Polymer based systems on tissue engineering, replacement and regeneration. NATO/ASI science series, Dordrecht: Kluwer; 2002.
[31] Tschoegl NW, The phenomenological theory of linear viscoelastic behavior, Berlin: Springer; 1989.
[32] Zoller P, Bolli P, Pahud V, Ackermann H. Rev Sci Instrum 1976;47: 948.
[33] Berry JM, Brostow W, Hess M, Jacobs EG. Polymer 1998;39:4081.
[34] Brostow W, Castaño VM, Martinez-Barrera G, Saiter J-M. Physica B. Submitted for publication.
[35] Nakagawa K, Ishida Y. J Polymer Sci Phys 1973;11:2153.
[36] Mano JF, Sousa RA, Reis RL, Cunha AM, Bevis MJ. Polymer 2001; 42:6187.
[37] Hartmann B, Haque MA. J Appl Phys 1985;58:2831.
[38] Hartmann B, Haque MA. J Appl Polymer Sci 1985;30:1553.
[39] Brostow W, Szymanski W. J Rheol 1986;30:877.
[40] Mano EB, Polimeros como materiais de engenharia, São Paulo: Edgard Blücher; 1996.
[41] Brostow W. In: Krieger RE, Malabar FL, editors. Science of materials. ; 1985. Brostow W. Einstieg in die moderne werkstoffwissenschaft. München: Hanser; 1985.
[42] Turner S. Creep of polymeric materials. In: Buschow KHJ, Cahn RW, Flemings MC, Ilschner B, Kramer EJ, Mahajan S, editors. Encyclopedia of materials: science and technology. Amsterdam: Elsevier; 2001.
[43] Doolitle AK. J Appl Phys 1951;22:1741.
[44] Moura Ramos JJ, Mano JF, Sauer BB. Polymer 1997;38:1081.
[45] Mijovic J, Sy JW, Kwei TK. Macromolecules 1997;30:3042.
[46] Sy JW, Mijovic J. Macromolecules 2000;33:933.
[47] Boyd RH. Polymer 1985;26:323.
[48] Boyd RH. Polymer 1985;26:1123.
[49] Mano JF, Sencadas V, Mello Costa A, Lanceros-Mendez S. Mater Sci Eng A. Accepted for publication.
[50] Hu W-G, Boeffel C, Schmidt-Rohr K. Macromolecules 1999;32:1611.
[51] Schmidt-Rohr K, Spiess HW. Macromolecules 1991;24:5288.
[52] Mano JF. Macromolecules 2001;34:8825.
[53] Lanceros-Mendez S, Mano JF, Medes JA. Ferroelectrics 2002;270: 271.
[54] McCrum NG, Read BE, Williams G. Anelastic and dielectric effects in polymeric solids. New York: Dover; 1991.